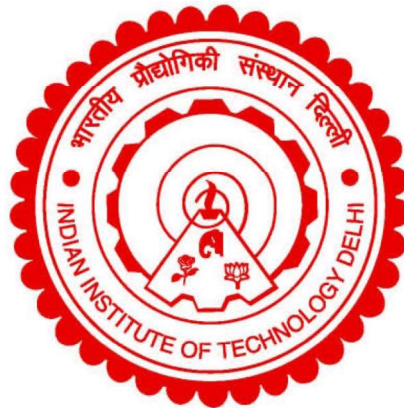


**DESIGN, DEVELOPMENT AND IMPLEMENTATION
OF BIDIRECTIONAL BATTERY CHARGERS OF
LIGHT ELECTRIC VEHICLES**

UTSAV SHARMA



**DEPARTMENT OF ELECTRICAL ENGINEERING
INDIAN INSTITUTE OF TECHNOLOGY DELHI**

JUNE 2025

© **Indian Institute of Technology Delhi (IITD), New Delhi, 2025**

**DESIGN, DEVELOPMENT AND IMPLEMENTATION
OF BIDIRECTIONAL BATTERY CHARGERS OF
LIGHT ELECTRIC VEHICLES**

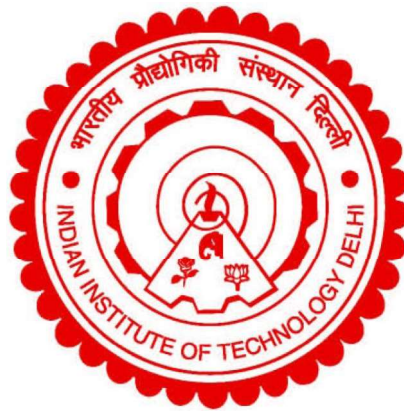
by

UTSAV SHARMA
Department of Electrical Engineering

Submitted

in fulfillment of the requirements of the degree of
DOCTOR OF PHILOSOPHY

to the



INDIAN INSTITUTE OF TECHNOLOGY DELHI
JUNE 2025

CERTIFICATE

It is certified that the thesis entitled “**Design, Development, and Implementation of Bidirectional Chargers for Light Electric Vehicle,**” being submitted by **Mr. Utsav Sharma** for an award of the degree of **Doctor of Philosophy** in the Department of Electrical Engineering, Indian Institute of Technology Delhi, is a record of the student work carried out by him under my supervision and guidance. The matter embodied in this thesis has not been submitted for any other degree or diploma award.

Dated: 30 June 2025

(Prof. Bhim Singh)

**Electrical Engineering Department
Indian Institute of Technology Delhi,
Hauz Khas, New Delhi-110016, India**

ACKNOWLEDGEMENT

I am deeply grateful to Prof. Bhim Singh for his steadfast guidance and supervision throughout my doctoral journey. Under his mentorship, my research experience has been profoundly enriched, offering me invaluable insights. Prof. Bhim Singh's unwavering determination, dedication, innovativeness, resourcefulness, and discipline have consistently inspired me, contributing significantly to the successful completion of this endeavor. His encouragement, meticulous oversight, and commitment to excellence have continually motivated me to strive for improvement and realize my full potential.

I extend sincere thanks to Prof. Bijay Ketan Panigrahi, Prof. Anandarup Das, Prof. Ashu Verma, Prof. G. Bhuvanewari, all members of the SRC for their invaluable guidance and unwavering support during my research. I also acknowledge the scholarly contributions of Prof. Bhim Singh, Prof. B. P. Singh, Prof. Amit Kumar Jain, and Late Prof. Mashuq-Un-Nabi during my coursework, which have laid a robust foundation for my research. The facilities provided by the Indian Institute of Technology Delhi are indispensable to my work, for which I am deeply appreciative.

Special gratitude is owed to Prof. Bhim Singh and Prof. M. Veerachary, as well as the staff of the PG Machine Lab, for their generous assistance with experimental facilities. I also recognize the support of Sh. Srichand, Sh. Puran Singh, Sh. Amit Kumar and Sh. Jitendra from various labs at IIT Delhi.

I am thankful to my seniors, colleagues, and friends who have supported me throughout this journey, including Dr. Ikhtlaq Hussain, Dr. Sachin Devassy, Dr. Aniket Anand, Dr. Nishant Kumar, Dr. Khusro Khan, Dr. Shadab Murshid, Dr. Anshul Varshney, Dr. Sreejith R, Dr. Saurabh Shukla, Dr. Shatakshi Jha, Dr. Shailendra Kumar Dwivedi, Dr. Piyush Kant, Dr. Seema Kewat, Dr. Radha Khushwaha, Dr. Priyank Mukeshkumar Shah, Dr. VL Srinivas, Dr. Anjeet Kumar Verma, Dr. Subarni Pradhan, Dr. Anjaneer Kumar Mishra, Dr. Deepu Vijay M, Dr. Utkarsh Sharma, Dr. Debasish Mishra, Dr. P. Sambasivaiah, Dr. Pavitra Shukl, Dr. Farheen Chishti, Dr. Rohini Sharma,

Dr. Mohd. Kashif, Dr. Hina Parveen, Dr. Aryadip Sen, Dr. Yalavarthi Amarnath, and others who provided both technical and non-technical assistance. I extend my sincere gratitude to Dr. Shailendra Kumar Dwivedi, Dr. Piyush Kant, Dr. Anjeet Verma, Dr. Utkarsh Sharma, Dr. Farheen Chishti, and Dr. Hina Parveen for their invaluable cooperation and informal support throughout the pursuit of this research work.

Special thanks are also due to Dr. Souvik Das, Dr. Jitendra Gupta, Dr. Gaurav Modi, Dr. Shalvi Tyagi, Dr. Syed Bilal Qaiser Naqvi, Dr. Sudip Bhattacharyya, Mr. Sandeep Kumar Sahoo, Dr. Yashi Singh, Dr. Cheshta Jain, Dr. Swagata Mapa and all colleagues who supported me.

Furthermore, I would like to express my gratitude to Dr. Vivek Narayanan, Dr. Saran Chaurasiya, Dr. Sayandev Ghosh, Dr. Suri Rama Naga Praneeth, Dr. Priyvratt Vats, Mr. Rahul Kumar, Mr. Sharankumar Shastri, Mr. Deepak Saw, Dr. Shivam Kumar Yadav, Mrs. Kousalya V, Dr. Sanjenbam Chandrakala Devi, Mr. Saurabh Mishra, Mr. Mohammad Junaid, Dr. Muhammad Zarkab Farqooi, Mrs. Kripa Tiwari, Dr. Rohit Kumar, Mr. Vipin Kumar Singh, Mr. Arjun Kumar, Mr. Biswajit Saha, Ms. Farha Siddique, Mr. Sumit Kumar, Mr. Gaurav Kumar, Mr. Himansu Sahoo, Mr. Adnan Farooq Khan, Mr. Chetan Shashank Matwankar, Ms. Smita Mohanty, and all members of the PG Machines lab group for their invaluable support.

Moreover, I would like to thank Department of Science and Technology (DST), Govt. of India for funding this research work under the fund for improvement of S&T infrastructure in higher educational institutions (FIST), Clean Energy (RP03195), J C Bose Fellowship (RP03128) and SERB NSC Fellowship.

I am profoundly grateful to my mother, Mrs. Ujjwal Pachauri, and my father, Mr. Vivek Kumar Sharma, for nurturing my dreams, showering me with their blessings, and always cheering me on. Their unwavering support has been my guiding light. My heartfelt thanks go to my beloved wife, Mrs. Anu, and our little son, Vidit Sharma, whose boundless love and unwavering encouragement

have been my source of strength throughout this journey. I am also deeply appreciative of my elder brother, Upwan Sharma, my sister-in-law, Mrs. Anam Naqvi, and my dear nephew, Vihan Sharma. Their steadfast support and belief in my abilities have been a constant inspiration and a cornerstone of my achievements.

Finally, I am thankful to the Almighty for granting me the strength, wisdom, and determination to achieve this significant academic milestone. I pray for continued guidance and blessings in all my future endeavors.

Dated: 30.06.2025

Utsav Sharma

ABSTRACT

The increasing demand for sustainable transportation solutions has significantly advanced research into bidirectional battery chargers for electric vehicles (EVs), with a particular focus on low-voltage battery-powered EVs, commonly referred to as light electric vehicles (LEVs). This thesis comprehensively explores various topologies and control strategies designed to enhance the efficiency and versatility of bidirectional chargers tailored specifically for LEVs.

The research begins with an extensive review of existing literature and market trends, highlighting the evolution and importance of bidirectional chargers in enabling vehicle-to-grid (V2G), vehicle-to-home (V2H), and other vehicle-to-anything (V2X) operations. It underscores state-of-the-art technologies and ongoing global projects that demonstrate the critical role bidirectional chargers play in integrating EVs with smart grids and smart homes.

Following this foundational review, the thesis delves into the design, development, and implementation of multiple bidirectional charger topologies. Key challenges addressed include ensuring wide-input voltage range operation, accommodating wide-output current range capabilities, and adapting to wide-output voltage ranges. Each topology is rigorously evaluated through detailed simulation analyses and practical hardware validations to ensure compliance with power quality standards and efficiency benchmarks. The integration of solar photovoltaic arrays with bidirectional chargers is also explored, expanding the scope of the research to address energy management challenges and promote sustainability in LEV operations. Additionally, the thesis investigates the feasibility of bridgeless bidirectional chargers, which aim to reduce component count and improve overall efficiency.

Through detailed chapters that provide theoretical insights, practical implementations, and performance evaluations, this research makes significant contributions to the advancement of bidirectional charger technology for LEVs. It highlights the adaptability and effectiveness of the developed chargers across a variety of operational scenarios.

In conclusion, the findings of this thesis underscore the efficacy and adaptability of the developed bidirectional chargers, laying a solid foundation for further research. They pave the way for optimizing the performance of bidirectional chargers, enhancing their integration into smart home ecosystems, and furthering sustainable transportation initiatives.

सारांश

सतत परिवहन समाधानों की बढ़ती माँग के कारण इलेक्ट्रिक वाहनों (EVs) के लिए bidirectional चार्जर्स पर हो रहा अनुसंधान तेज़ी से आगे बढ़ा है, विशेषकर उन वाहनों के लिए जो कम वोल्टेज बैटरियों पर चलते हैं, जिन्हें *लाइट इलेक्ट्रिक व्हीकल्स (LEVs)* कहा जाता है। यह शोध प्रबंध LEVs के लिए उपयुक्त bidirectional चार्जर्स की दक्षता और बहुपरिप्रेक्ष्यता बढ़ाने हेतु विभिन्न टोपोलॉजी और नियंत्रण विधियों का समग्र अध्ययन प्रस्तुत करता है।

शोध की शुरुआत मौजूदा साहित्य और बाज़ार प्रवृत्तियों की विस्तृत समीक्षा से होती है, जिसमें यह स्पष्ट किया गया है कि bidirectional चार्जर किस प्रकार V2G (Vehicle-to-Grid), V2H (Vehicle-to-Home) और V2X (Vehicle-to-Anything) जैसे अनुप्रयोगों को संभव बनाते हैं। साथ ही, यह अध्ययन उन नवीनतम तकनीकों और वैश्विक परियोजनाओं पर भी प्रकाश डालता है जो EVs को स्मार्ट ग्रिड और स्मार्ट होम्स से एकीकृत करने में मदद कर रही हैं।

इसके पश्चात, शोध विभिन्न bidirectional चार्जर टोपोलॉजी के डिज़ाइन, विकास और कार्यान्वयन पर केंद्रित है। इसमें प्रमुख तकनीकी चुनौतियों — जैसे विस्तृत इनपुट वोल्टेज रेंज, आउटपुट करंट और वोल्टेज रेंज में अनुकूलता — को संबोधित किया गया है। सभी टोपोलॉजी का मूल्यांकन गहन सिमुलेशन और प्रयोगात्मक हार्डवेयर परीक्षणों के माध्यम से किया गया है, ताकि यह सुनिश्चित किया जा सके कि वे पावर क्वालिटी मानकों और दक्षता मापदंडों पर खरी उतरें।

इसके अतिरिक्त, सौर फोटावोल्टिक (PV) प्रणाली के साथ bidirectional चार्जर्स के एकीकरण की संभावनाओं का भी अध्ययन किया गया है, जो ऊर्जा प्रबंधन और स्थायित्व की दिशा में एक सकारात्मक कदम है। साथ ही, ब्रिजलेस bidirectional चार्जर की संभाव्यता पर भी शोध किया गया है, जिनका उद्देश्य घटकों की संख्या को कम कर दक्षता में सुधार लाना है।

इस शोध के विभिन्न अध्यायों में सैद्धांतिक अवधारणाएं, व्यावहारिक कार्यान्वयन, और प्रदर्शन मूल्यांकन शामिल हैं, जो LEVs के लिए bidirectional चार्जर तकनीक के विकास में उल्लेखनीय योगदान प्रदान करते हैं। यह शोध विभिन्न परिचालन परिदृश्यों में विकसित चार्जर्स की अनुकूलता और प्रभावशीलता को रेखांकित करता है।

अंततः, यह शोध प्रबंध यह सिद्ध करता है कि विकसित bidirectional चार्जर न केवल प्रभावी हैं, बल्कि भविष्य के अनुसंधान, स्मार्ट होम इंटीग्रेशन और सतत परिवहन पहलों के लिए एक सशक्त आधार भी प्रदान करते हैं।

TABLE OF CONTENTS

	Page No.
Certificate	i
Acknowledgement	ii
Abstract	v
Table of Contents	vii
List of Figures	xvi
List of Tables	xx
List of Abbreviations	xxi
List of Variables	xxiii
CHAPTER - I INTRODUCTION	
1.1 General	1
1.2 Bidirectional Battery Charger Technology	2
1.2.1 Classification of Battery Chargers	3
1.2.2 Classification of Bidirectional Operation	4
1.3 Existing Bidirectional Battery Chargers in Market	5
1.4 Existing LEVs in the Market	6
1.5 State-of-Art on Bidirectional Battery Chargers	8
1.6 Scope of Work	11
1.7 Thesis Organization	14
CHAPTER - II LITERATURE REVIEW	
2.1 General	20
2.2 Literature Survey	21
2.2.1 Review of Configurations for Bidirectional Battery Charger with Wide-input Voltage Range Operation	21
2.2.2 Review of Configurations for Bidirectional Battery Charger with Wide-output Current Range Operation	26
2.2.3 Review of Configurations for Bidirectional Battery Charger with Wide-output Voltage Range Operation	28
2.2.4 Review of Configurations for Bidirectional Battery Charger for Solar Photovoltaic Array Equipped LEVs	30
2.2.5 Review of Bridgeless Bidirectional Battery Chargers for LEVs	31
2.3 Identified Research Areas	33
2.4 Summary	35

CHAPTER - III DESIGN, DEVELOPMENT AND IMPLEMENTATION OF BIDIRECTIONAL BATTERY CHARGER WITH WIDE-INPUT VOLTAGE RANGE OPERATION

3.1	General	36
3.2	Configuration of Bidirectional Charger with capability of Wide-Input Voltage Range Operation	36
3.2.1	Configuration of Interleaved Synchronous Buck Converter based Bidirectional Charger	37
3.2.2	Configuration of Dual Active Bridge Converter based Bidirectional Charger	38
3.3	Design of Bidirectional Charger with Capability of Wide-Input Voltage Range Operation	38
3.3.1	Design of Bidirectional AC/DC converter	38
3.3.2	Design of Interleaved Synchronous Buck Converter	40
3.3.3	Design of Dual Active Bridge Converter	40
3.4	Control of Bidirectional Charger with Capability of Wide-Input Voltage Range Operation	42
3.4.1	Control Algorithm for Interleaved Synchronous Buck Converter Based Bidirectional Charger	42
3.4.2	Control Algorithm for DAB Converter Based Bidirectional Charger	48
3.5	MATLAB Based Modelling and Simulation of Bidirectional Charger with Capability of Wide-Input Voltage Range Operation	52
3.6	Hardware Implementation of Bidirectional Charger	52
3.6.1	Hardware Implementation of i-SB Converter Based Bidirectional Charger	53
3.6.2	Hardware Implementation of DAB Converter Based Bidirectional Charger	57
3.7	Results and Discussion	57
3.7.1	Simulation Analysis of i-SB Converter Based Bidirectional Charger	58

3.7.2	Simulation Analysis of DAB Converter Based Bidirectional Charger	60
3.7.3	Experimental Performance of Interleaved Synchronous Buck Converter based Bidirectional Charger	61
3.7.3.1	Performance of Charger with Universal AC Supply	62
3.7.3.2	Frequency Estimation Performance of Charger	64
3.7.3.3	Performance of Charger at Distorted Grid Voltage	65
3.7.3.4	Performance of Charger during V2G operation	67
3.7.3.5	Steady-State Performance of i-SB Converter under Rated Operating Condition	68
3.7.4	Experimental Results of Dual Active Bridge Converter based Bidirectional Charger	69
3.7.4.1	Performance of Charger with Universal AC Supply	69
3.7.4.2	Performance of Charger at Distorted Grid Voltage	72
3.7.4.3	Performance of Charger during V2G operation	74
3.7.4.4	Steady-state performance of i-SB converter under rated operating condition	75
3.8	Summary	77
CHAPTER - IV DESIGN, DEVELOPMENT AND IMPLEMENTATION OF BIDIRECTIONAL BATTERY CHARGERS WITH WIDE-OUTPUT CURRENT RANGE OPERATION		
4.1	General	79
4.2	Configuration of Bidirectional Charger with capability of Wide-Output Current Range Operation	80
4.2.1	Configuration of Switched-Inductor derived SEPIC Converter Based Bidirectional Charger	80
4.2.2	Configuration of Isolated Interleaved SEPIC Converter based Bidirectional Charger	81
4.3	Design of Bidirectional Charger	81
4.3.1	Design of Bidirectional AC/DC converter	82

4.3.2	Design of SI-SEPIC Converter	82
4.3.3	Design of ii-SEPIC Converter	84
4.4	Control of Bidirectional Charger with Capability of Wide-Output Current Range Operation	85
4.4.1	Control Algorithm for SI-Sepic Converter Based Bidirectional Charger	85
4.4.2	Control Algorithm for ii-Sepic Converter Based Bidirectional Charger	87
4.5	MATLAB based Modeling and Simulation of Bidirectional Charger with Capability of Wide-Output Current Range Operation	92
4.6	Hardware Implementation of Bidirectional	93
4.6.1	Hardware Implementation of SI-Sepic Converter Based Bidirectional Charger	93
4.6.2	Hardware Implementation of ii-Sepic Converter Based Bidirectional Charger	94
4.7	Results and Discussion	95
4.7.1	Simulation Analysis of SI-Sepic Converter Based Bidirectional Charger Simulation	95
4.7.1.1	Performance of Charger with Multistep Constant Current Charging Operation	95
4.7.1.2	Performance of Charger Under Varying Grid Voltage Condition	96
4.7.1.3	Performance of Charger During Vehicle to Grid operation	97
4.7.1.4	Steady-state Performance of SI-SEPIC Converter at Rated Condition	98
4.7.2	Simulation Analysis of ii-Sepic Converter Based Bidirectional Charger Simulation	98
4.7.2.1	Performance of Charger with Multistep Constant Current Charging Operation	99
4.7.2.2	Performance of Charger Under Varying Grid Voltage Condition	99
4.7.2.3	Performance of Charger During Vehicle to Grid operation	100

4.7.2.4	Steady-state Performance of ii-SEPIC Converter at Rated Condition	101
4.7.3	Experimental Results of SI-SEPIC Converter Based Bidirectional Charger	101
4.7.3.1	Steady State Charging Performance	102
4.7.3.2	Performance during Wide Output Current Range Variation	103
4.7.3.3	Performance during Varying Grid Voltage	105
4.7.3.4	Performance during V2G Operation	107
4.7.3.5	Voltage Stress across Switches of SI-SEPIC Converter	109
4.7.4	Experimental Results of ii-SEPIC Converter based Bidirectional Charger	110
4.7.4.1	Steady State Charging Performance	110
4.7.4.2	Performance during Wide Output Current Range Variation	112
4.7.4.3	Performance during Varying Grid Voltage	113
4.7.4.4	Performance during V2G Operation	115
4.7.4.5	Voltage Stress across Switches of ii-SEPIC Converter	118
4.8	Summary	118

CHAPTER - V DESIGN, DEVELOPMENT, AND IMPLEMENTATION OF BIDIRECTIONAL BATTERY CHARGERS WITH WIDE-OUTPUT VOLTAGE RANGE OPERATION

5.1	General	120
5.2	Configuration of Bidirectional Charger with capability of Wide-Output Voltage Range Operation	120
5.2.1	Configuration of Isolated Cuk Converter based Bidirectional Charger	121
5.2.2	Configuration of Isolated Cuk Converter based Bidirectional Charger	121
5.3	Design of Bidirectional Charger	122
5.3.1	Design of Bidirectional AC/DC converter	122
5.3.2	Design of SC-SEPIC Converter	122
5.3.3	Design of Isolated Cuk Converter	125
5.4	Control of Bidirectional Charger with Capability of Wide-Output Voltage Range Operation	126

5.4.1	Control Algorithm For SC-SEPIC Converter Based Bidirectional Charger	127
5.4.2	Control Algorithm For CI-CUK Converter Based Bidirectional Charger	130
5.5	MATLAB based Modeling and Simulation of Bidirectional Charger with Capability of Wide-Output Voltage Range Operation	134
5.6	Hardware Implementation of Bidirectional Charger with Capability of Wide-Output Voltage Range Operation	134
5.6.1	Hardware Implementation of SC-SEPIC Converter Based Bidirectional Charger	135
5.6.2	Hardware Implementation of CI-CUK Converter Based Bidirectional Charger	136
5.7	Results and Discussion	137
5.7.1	Simulation Analysis of SC-SEPIC Based Bidirectional Charger	137
5.7.1.1	Switch Voltage Stress Verification during Charging Operation of a 48 V Battery	137
5.7.1.2	Performance of Charger during Wide Output Voltage Operation	137
5.7.1.3	Performance of Charger during varying grid voltage operation	140
5.7.1.4	Performance of Charger during V2G Operation	140
5.7.2	Simulation Analysis of CI-CUK converter Based Bidirectional Charger	141
5.7.2.1	Switch Voltage Stress Verification during Charging Operation of a 48 V Battery	141
5.7.2.2	Performance of Charger during Wide Output Voltage Operation	142
5.7.2.3	Performance of Charger during varying grid voltage operation	144
5.7.2.4	Performance of Charger during V2G Operation	144
5.7.3	Experimental Performance of SC-SEPIC Based Bidirectional Charger	145

5.7.3.1	Performance of Charger during Wide Output Voltage Operation	145
5.7.3.2	Performance of Charger during varying grid voltage operation	148
5.7.3.3	Performance of Charger during V2G Operation	149
5.7.4	Experimental Performance of CI-CUK Converter Based Bidirectional Charger	151
5.7.4.1	Performance of Charger during Wide Output Voltage Operation	151
5.7.4.2	Performance of Charger during varying grid voltage operation	154
5.7.4.3	Performance of Charger during V2G Operation	156
5.8	Summary	158

CHAPTER - VI DESIGN, DEVELOPMENT AND IMPLEMENTATION OF BIDIRECTIONAL BATTERY CHARGER FOR SOLAR PHOTOVOLTAIC ARRAY EQUIPPED LEVS

6.1	General	159
6.2	Configuration of Bidirectional Charger for Solar Photovoltaic Array Equipped LEVs	160
6.3	Design of Bidirectional Charger for Solar Photovoltaic Array Equipped LEVs	161
6.3.1	Design of Bidirectional AC/DC converter	161
6.3.2	Design of CI-Cuk Converter	161
6.3.3	Design of Boost converter for Maximum Power Point Tracking of SPV Array	161
6.4	Control of Bidirectional Charger for SPV Array Equipped LEVs	161
6.4.1	Control Algorithm of VSC	161
6.4.2	Control Algorithm of CI-Cuk Converter	166
6.4.3	Control Algorithm of Boost converter	167
6.5	MATLAB based Modeling and Simulation of Bidirectional Charger	168
6.6	Hardware Implementation of Bidirectional Charger for Solar Photovoltaic Array Equipped LEVs	168
6.7	Results and Discussion	169

6.7.1	Simulation Analysis of Charging Operation during Absence of Grid-connection	169
6.7.2	Simulation Analysis of Grid Connected Mode Charging Operation	170
6.7.3	Simulation Analysis of V2G Mode	171
6.7.4	Experimental Performance of Charging Operation during Absence of Grid Supply	171
6.7.5	Experimental Performance of Grid Connected Mode Charging Operation	174
6.7.6	Experimental Performance of V2G Mode	182
6.8	Summary	184
CHAPTER - VII DESIGN, DEVELOPMENT AND IMPLEMENTATION OF BRIDGELESS BIDIRECTIONAL BATTERY CHARGERS FOR LEVS		
7.1	General	185
7.2	Configuration of Bridgeless Bidirectional Battery Charger	185
7.3	Design of Bidirectional Charger	186
7.3.1	Estimation of Operating Range of Duty Cycle	192
7.3.2	Estimation of Inductances of Charger	193
7.3.3	Estimation of Capacitors of Charger	194
7.3.4	Estimation of Voltage Stress across Capacitors	195
7.3.5	Estimation of Voltage Stress across Switches	195
7.4	Control of Bridgeless Bidirectional Charger	196
7.4.1	Grid to Vehicle Mode Control	196
7.4.2	Vehicle to Load Mode Control	197
7.5	MATLAB Based Modelling and Simulation of Bidirectional Charger	197
7.6	Hardware Implementation of Bidirectional Charger	198
7.7	Results and Discussion	198
7.7.1	Simulation Analysis of Bridgeless Bidirectional Charger	198
7.7.2	Experimental Analysis of Bridgeless Bidirectional Charger	201
7.7.2.1	Steady-State Performance Analysis during G2V Operation	201
7.7.2.2	Voltage and Current Stress of the Charger's Components	203
7.7.2.3	Dynamic Performance Analysis during G2V Operation	205
7.7.2.4	Performance Analysis during V2L Operation	206
7.8	Summary	207

CHAPTER - VIII	MAIN CONCLUSIONS AND SUGGESTIONS FOR FURTHER WORK	
8.1	General	208
8.2	Main Conclusions	209
8.3	Suggestions for Further Work	214
	REFERENCES	216-222
	LIST OF PUBLICATIONS	223-224
	BIO-DATA	225

LIST OF FIGURES

- Fig. 1.1 Schematic of two-stage bidirectional battery charger
- Fig. 1.2 Schematic of DAB converter-based topology for bidirectional battery charger
- Fig. 1.3 Schematic of Matrix converter-based topology for bidirectional battery charger
- Fig. 3.1 Configuration of (a) synchronous buck converter-based charger, and (b) interleaved synchronous buck converter-based charger
- Fig. 3.2 Schematic of DAB converter based bidirectional charger
- Fig. 3.3 Block diagram of AL-QSG based FLL
- Fig. 3.4 Control scheme of VSC
- Fig. 3.5 Control scheme of i-SBDC converter
- Fig. 3.6 Block diagram of (a) controller for VSC and frequency analysis of transfer functions G_p and G_q of m-MFV (b)-(c) with variation in α and (d)-(e) with variation in k
- Fig. 3.7 Control block diagram for DAB converter
- Fig. 3.8 Simulation diagram of (a) i-SB converter based charger and (b) DAB converter based charger
- Fig. 3.9 Experimental setup for i-SB converter based bidirectional battery charger with i-SB converter
- Fig. 3.10 Photograph of LEM-LA100P Hall Effect current sensor and circuit diagram of current sensor board.
- Fig. 3.11 Photograph of LEM LV-25 Hall Effect voltage sensor and circuit diagram of voltage sensor board.
- Fig. 3.12 Photograph of opto-isolation board and its circuit layout.
- Fig. 3.13 Experimental setup for DAB converter-based bidirectional battery charger
- Fig. 3.14 Simulation analysis of i-SB converter based charger in varying operation scenarios
- Fig. 3.15 Voltage stress across switches and current stress across inductors of i-SB converter in developed charger
- Fig. 3.16 Simulation analysis of DAB converter-based charger in varying operation scenarios
- Fig. 3.17 Voltage stress across switches and current stress across inductors of DAB converter in developed charger
- Fig. 3.18 Battery charger operation with wide grid voltage variation
- Fig. 3.19 Steady-state performance of i-SB converter based bidirectional battery charger during wide grid voltage range
- Fig. 3.20 Experimental comparison of frequency estimation performance
- Fig. 3.21 Results amid charging of a battery when grid voltage is distorted
- Fig. 3.22 Power quality results amid operation at distorted grid voltage
- Fig. 3.23 (a) Dynamic behavior of charger, (b) grid voltage and current value, (c) UPF operation, and (d) IEC compliance supporting results amid V2G operation
- Fig. 3.24 Voltage stress across switches and current stress across inductors of i-SB converter in developed charger

Fig. 3.25	Battery charger operation with wide grid voltage variation
Fig. 3.26	Steady-state performance of DAB converter based bidirectional battery charger during wide grid voltage range
Fig. 3.27	Power quality results amid operation at distorted grid voltage
Fig. 3.28	(a) Dynamic behavior of charger, (b) grid voltage and current value, (c) UPF operation, and (d) IEC compliance supporting results amid V2G operation
Fig. 3.29	Result of DAB converter during the steady-state operation
Fig. 4.1	Configuration of switched-inductor derived SEPIC based bidirectional charger
Fig. 4.2	Schematic of ii-SEPIC converter based bidirectional charger
Fig. 4.3	Diagrams depicting control of a VSC
Fig. 4.4	Diagrams depicting control of SI-SEPIC
Fig. 4.5	Block diagram of (a) VSC control unit with FLNN-assisted DPCC, and (b) SOGI-PLL for unit template generation
Fig. 4.6	Block diagram of ii-SEPIC control unit
Fig. 4.7	Simulation diagram of (a)SI-SEPIC converter-based charger and (b) ii-SEPIC converter based charger
Fig. 4.8	Experimental circuit for validation of SI-SEPIC converter based charger's operation
Fig. 4.9	Experimental circuit for validation of ii-SEPIC converter based charger's operation
Fig. 4.10	Simulation analysis of SI-SEPIC converter-based charger
Fig. 4.11	Voltage and current stress analysis of SI-SEPIC converter during the charging operation
Fig. 4.12	Simulation analysis of ii-SEPIC converter-based charger
Fig. 4.13	Voltage and current stress of switches in one cell of ii-SEPIC converter during charging operation
Fig. 4.14	Results during rated condition of charging
Fig. 4.15	Grid voltage, current and power quality at rated charging operation
Fig. 4.16	Multistep charging operation of the charger
Fig. 4.17	Grid voltage, current and power quality at reduced load operation
Fig. 4.18	Results amid varying grid voltage condition
Fig. 4.19	Steady-state results amid varying grid voltage condition
Fig. 4.20	Results amid V2G operation
Fig. 4.21	Experimental results of SI-SEPIC converter during rated operation
Fig. 4.22	Results during rated condition of charging
Fig. 4.23	Grid voltage, current and power quality at rated charging operation
Fig. 4.24	Multistep charging operation of the charger
Fig. 4.25	Grid voltage, current and power quality at reduced load operation
Fig. 4.26	Charging during varying voltage condition
Fig. 4.27	Steady state results during the (a)-(c) voltage sag operation and (d)-(f) voiltage swell operation
Fig. 4.28	Experimental results for V2G operation
Fig. 4.29	Grid side results during V2G operation

- Fig. 4.30 Experimental results of one ii-SEPIC converter's cell during rated operation
- Fig. 5.1 Configuration of SC-SEPIC based bidirectional charger
- Fig. 5.2 Schematic of CI-Cuk converter based bidirectional charger
- Fig. 5.3 Diagram of (a) VSC control unit, with (b) SOGI-FLL
- Fig. 5.4 Diagram of modified SEPIC control unit
- Fig. 5.5 Block diagram of HFLNN-DPCC based control unit of VSC
- Fig. 5.6 CI-Cuk converter's control block diagram
- Fig. 5.7 MATLAB Simulink diagram of (a) SC-SEPIC-based charger and (b) CI-Cuk converter-based charger
- Fig. 5.8 Hardware test-bench for experimental analysis of SC-SEPIC converter-based battery charger
- Fig. 5.9 Experimental setup for CI-Cuk converter-based battery charger
- Fig. 5.10 Simulation result of SC-SEPIC based charger with 48 V battery
- Fig. 5.11 Simulation result of SC-SEPIC based charger with varying input voltage supply
- Fig. 5.12 Simulation result of SC-SEPIC based charger with (a) 120 V battery, (b) V2G operation with 48 V battery
- Fig. 5.13 Simulation result of CI-Cuk Converter based charger with 48 V battery
- Fig. 5.14 Simulation result of CI-Cuk Converter based charger with varying input voltage supply
- Fig. 5.15 Simulation result of CI-Cuk Converter based charger with (a) 120 V battery, (b) V2G operation with 48 V battery
- Fig. 5.16 Steady-state result of SC-SEPIC based charger battery charger during charging of a 48 V battery
- Fig. 5.17 Grid side performance of battery charger while the charging of a 48 V battery
- Fig. 5.18 Charging a 120 V battery with 7 A battery current using a 230 V, 50 Hz AC supply
- Fig. 5.19 Operation of battery charger showing (a) dynamic performance, (b)-(g) grid current quality during voltage swell and sag conditions
- Fig. 5.20 V2G operation of battery charger with SC-SEPIC based charger showing (a) smooth change in battery current direction, (b) grid voltage and current waveforms, (c) power factor, and (d) THD of grid current
- Fig. 5.21 Experimental result of charging a 48 V battery with CI-Cuk converter-based charger
- Fig. 5.22 Steady-state results during 48 V battery charging with CI-Cuk converter based charger
- Fig. 5.23 Experimental result of charging a 120 V battery with CI-Cuk converter-based charger
- Fig. 5.24 Experimental results during (a) voltage sag condition, and (b) voltage swell condition
- Fig. 5.25 V2G operation of battery charger with CI-Cuk converter based charger showing grid current quality during voltage sag and swell conditions
- Fig. 5.26 Key waveforms during the (a)V2G operation, and (b)-(d) grid current quality results
- Fig. 6.1 Circuit diagram of bidirectional battery chargers with SPV-array
- Fig. 6.2 VSC control block diagram

- Fig. 6.3 CI-Cuk converter's control block diagram
- Fig. 6.4 MATLAB-Simulink Model of multi-objective bidirectional charger
- Fig. 6.5 Laboratory test-bench set-up
- Fig. 6.6 Simulation result under (a) islanded mode and (b) grid-connected mode in presence of solar power (c) change in battery current amid charging and (d) V2G operation
- Fig. 6.7 Experimental results during vehicle-in-move mode of operation.
- Fig. 6.8 Experimental results of MPPT operation of SPV array in an LEV with (a) 1000 W/m^2 , and (d) 400 W/m^2
- Fig. 6.9 Dynamic performance when grid current reduces
- Fig. 6.10 Grid side waveforms at rated load operation (a)-(c), and at reduced load operation (d)-(f)
- Fig. 6.11 Dynamic behavior of presented battery charger during (a) grid voltage sag and (b) grid voltage swell
- Fig. 6.12 Steady-state analysis during G2V operation at grid voltage (a)-(c) sag, and (d)-(f) swell event
- Fig. 6.13 Resulting waveforms of battery charger operation at distorted grid
- Fig. 6.14 Stead-state results of battery charger operation at distorted grid
- Fig. 6.15 Results of battery charger amid V2G operation
- Fig. 7.1 Circuit diagram of bridgeless bidirectional battery charger
- Fig. 7.2 Operating modes of EV charger amid the charging operation (a)-(c) during positive half cycle, and (d)-(f) during negative half cycle of grid voltage
- Fig. 7.3 Key waveforms of operating conditions
- Fig. 7.4 Operating modes of EV charger amid V2H operation (a)-(c) during positive half cycle, and (d)-(f) during negative half cycle of AC voltage.
- Fig. 7.5 Control block diagram
- Fig. 7.6 MATLAB-Simulink Model of bridgeless bidirectional charger
- Fig. 7.7 Laboratory test-bench set-up of multi-objective bidirectional charger
- Fig. 7.8 Simulation results
- Fig. 7.9 During G2V operation: (a) Charger's key waveforms, (b) grid voltage and current with RMS values, (c) UPF operation and power transferred under steady-state, and (d) grid current's THD with harmonic spectrum
- Fig. 7.10 Voltage stress across switches, S_1 , S_3 , Q_1 and Q_2 , and their zoom view
- Fig. 7.11 Voltage and current stress across (a) capacitors and (b) inductors respectively and their zoom view
- Fig. 7.12 Charger's operation under universal voltage supply range
- Fig. 7.13 V2L operation with developed charger

LIST OF TABLES

Table 1.1	Categorization of Battery Charger
Table 1.2	A List of Prominent Bidirectional Chargers Available in Market
Table 1.3	A List of Prominent LEV Manufacturers with Battery Rating of Their Flagship Product
Table 1.4	Worldwide Projects Related to Bidirectional Operation of Battery Charger
Table 3.1	Parameters for Battery Charger
Table 3.2	Estimated Parameter of Bidirectional Battery Charger
Table 3.3	Selected Control parameters for DISM Controller
Table 4.1	Parameters for Battery Charger
Table 4.2	Values of 'k' under distinct scenerios
Table 5.1	Parameters for Battery Charger
Table 5.2	Selected parameters for obc
Table 6.1	Parameter Used For Design of Bidirectional Battery Charger
Table 6.2	Estimated Parameter of Bidirectional Battery Charger
Table 7.1	Parameter Used For Design of Bidirectional Battery Charger

LIST OF ABBREVIATIONS

AL-QSG	Adaptive Lyapunov Quadrature Signal Generator
CAGR	Compounded Annual Growth Rate
CC	Constant Current
CCCV	Constant Current Constant Voltage
CCM	Continuous Conduction Mode
CF	Crest Factor
CI-Cuk	Coupled Inductor Cuk
CSOGI	Cascaded Second-Order Generalized Integrator
CV	Constant Voltage
DAB	Dual Active Bridge
DCM	Discontinuous Conduction Mode
DER	Distributed Energy Resource
DF	Distortion Factor
DISM	Double Integral Sliding Mode
DISMC	Double Integral Sliding Mode Control
DPCC	Deadbeat Predictive Current Control
DPF	Displacement Power Factor
DSC	Delay Signal Cancellation
DSP	Digital Signal Processor
E2W	Electric Two-Wheeler
E3W	Electric Three-Wheeler
EV	Electric Vehicle
FEC	Front End Converter
FLL	Frequency-Locked Loop
FLNN	Functional Link Neural Network
G2V	Grid To Vehicle
GCC	Grid-Connected Converter
Htan-PLL	Half-Tangent Phase-Locked Loop
HVCR	High Voltage Conversion Ratio
IEC	International Electrochemical Commission
IEEE	International Electrical And Electronics Engineering
IGBT	Insulated Gate Bipolar Transistor
ii-SEPIC	Isolated Interleaved Single-Ended Primary-Inductor Converter
i-SB	Interleaved Synchronous Buck
LD	Lyapunov's Demodulator
LEV	Light Electric Vehicle
LMS	Least Mean Square
LPF	Legendre Polynomial Function
L-QSG	Lyapunov Quadrature Signal Generator
MAF	Moving Average Filter
m-MVF	Modified Multivariable Filter
MPP	Maximum Power Point
MPPT	Maximum Power Point Tracking
MSCC	Multi Step Constant Current
MSOGI	Multilayer Second-Order Generalized Integrator
NEMA	National Manufacturers Association
NLF-PLL	Nonlinear Loop Filter-Based PLL
OEM	Original Equipment Manufacturer

PCC	Point Of Common Coupling
PF	Power Factor
PFC	Power Factor Correction
PI	Proportional Integral
PLL	Phase-Locked Loop
PR	Proportional Resonant
PWM	Pulsewidth Modulation
RMS	Root Mean Square
SAE	
SC	Switched Capacitor
SC-SEPIC	Switched Capacitor Single-Ended Primary-Inductor Converter
SEPIC	Single-Ended Primary-Inductor Converter
SI	Switched Inductor
SI-SEPIC	Switched Inductor Single-Ended Primary-Inductor Converter
SOGI	Second-Order Generalized Integrator
SPR	Strictly Positive Real
SPS	Single-Phase Shift
SPV	Solar Photovoltaic
THD	Total Harmonic Distortion
UPF	Unity Power Factor
V2G	Vehicle To Grid
V2H	Vehicle To Home
V2L	Vehicle To Load
V2V	Vehicle To Vehicle
VSC	Voltage Source Converter

LIST OF VARIABLES

Δi_g	Allowable ripples in grid current in one switching cycle
Δi_{L1}	Allowable ripple in inductor L_1
C	Constant matrix calculated from frequency of grid voltage
C_1	Capacitor in SEPIC/Cuk converter
C_1, C_2	Capacitors of bridgeless bidirectional converter
C_{DC}	DC link capacitor
C_{i1}, C_{i2}	Primary side capacitors of isolated SEPIC/Cuk converter
C_o	Output capacitor of DC/DC converter
C_{o1}, C_{o2}	Secondary side capacitors of isolated SEPIC/Cuk converter
D	Duty ratio of DC/DC converter
D	Duty ratio of non-isolated DC/DC converter
d	Control law for switching of VSC
D_1, D_2	Fraction of discharging time of output inductors
D_{max}	Maximum duty ratio of DC/DC converter
D_{min}	Minimum duty ratio of DC/DC converter
D_n	Nominal duty ratio of DC/DC converter
E	Disturbance matrix
e	General error signal
e_i	Current error between measured and reference grid current
e_l	Current error between measured and reference battery current
$f(x)$	State matrix function of input variable in state-space equation
$f_{cut-off}$	Cut-off frequency of the low pass filter
f_g	Grid frequency in Hz
f_s	Switching frequency of DC/DC converter
f_{sw}	Switching frequency of VSC
$g(x)$	Input matrix function of input variable in state-space equation
G_p and G_q	transfer functions of m-MVF
I	Identity matrix
I_{AUX}	Current to auxiliary loads in LEV
I_b	Battery current
$I_{b,err}$	Error in measured and reference battery current
$I_{b,ref}$	Reference battery current
I_{b1}	Charging current in provided by available solar power
I_{b2}	Charger's output current in SPV assisted battery charger
i_{C1}, i_{C2}	Current through capacitors C_1 and C_2
i_g	Grid current
$i_{g,err}$	Error in measured and reference grid current
$i_{g,r}$	Reference grid current
$I_{g,r}$	Intermediate grid reference current amplitude
$i_{g,ref}$	Reference grid current
I_i	Amplitude of grid current reference value
i_{Lin}	Current through inductors L_{in}
i_{Lo1} and i_{Lo2}	Current through inductors L_{o1} and L_{o2}
I_p	Current from SPV array
i_r	Amplitude of the grid reference current
I_{SP}	Battery current reference value
k	Battery current amplitude multiplier constant
k_1, k_2, k_3	Sliding mode controller constants

K_I	Integral constant in voltage controller of VSC
k_i	m-MVF multiplication factor
K_{II}	Integral constant in current controller of DC/DC convertor
k_m, α_m	m-MVF control variables
K_p	Proportional constant in voltage controller of VSC
K_{PI}	Proportional constant in current controller of DC/DC convertor
K_{VI}	Integral constant in voltage controller of DC/DC convertor
K_{VP}	Proportional constant in voltage controller of DC/DC convertor
L_i	Interfacing inductor of VSC
L_{i1}, L_{i2}	Input inductors of DC/DC converter
L_{in}	Input inductor of bridgeless bidirectional converter
L_{m1}, L_{m2}	Magnetizing inductance of transformer of isolated DC/DC converter
L_o	Equivalent output inductor of the DAB
L_{o1}, L_{o2}	Output inductors of DC/DC converter
L_s	Inductor in series with primary winding of an isolated DC/DC converter
m	Modulation factor
M	Mutual inductance
N	Transformer ratio
$P_1/P_2/P_3/P_4$	Switching signals to Primary side switches of isolated DC/DC converter
P_o	Power transfer capacity of DC/DC converter
P_p	Calculated PV power at SPV array terminal
$Q_1/Q_2/Q_3/Q_4$	Switching signals to secondary side switches of isolated DC/DC converter
r	Coupling coefficient
r_f-C_f	RC filter
R_o	Equivalent output resistance of the DAB
S	Sliding surface
$S_1/S_2/S_3/S_4$	Switching signal to VSC switches
T_o	Cycle time of input signal
T_s	Sampling period for FLNN algorithm
u	Input variable matrix in state-space equation
u_t	Unit template of the grid voltage
v_g	Grid voltage
V_b	Battery voltage
$V_{b,err}$	Error in measure and reference battery voltage
$V_{b,ref}$	Reference battery voltage
v_{C1}, v_{C2}	Instantaneous voltage across capacitors C_1 and C_2
V_{C1}, V_{C2}	Average voltage across capacitors C_1 and C_2
V_{DC}	DC link voltage
$V_{DC,err}$	Error in measured and reference DC link voltage
v_e	Reconstructed/calculated grid voltage
V_{Lin}	Voltage across inductor L_{in}
V_m	Amplitude of grid voltage
$V_{m,e}$	Estimated amplitude of grid voltage
V_p	SPV array terminal voltage
V_{PCC}	Voltage across point of common coupling
$V_{Q1}, V_{Q2}, V_{Q3}, V_{Q4}$	Voltage across switches $Q_1, Q_2, Q_3,$ and Q_4
V_{ref}	Reference DC link voltage

v_{rip}	Ripple in DC link voltage
v_{α}, v_{β}	Quadrature component of the grid voltage
x	Input variable matrix of a generalized state-space equation
y	Output variable matrix of a generalized state-space equation
Z	Impedance of the transformer in DAB
α	Ratio of the inductance considered in control algorithm to actual inductance
γ	Frequency multiplier factor
δ	Phase shift angle
$\Delta i_{Li1}, \Delta i_{Li2}$	Ripples in input inductor current
Δi_{Lm}	Ripples in magnetizing inductance
$\Delta i_{Lo1}, \Delta i_{Lo2}$	Ripples in output inductor current
ΔI_p	Change in SPV array output current
δ_{nom}	Nominal phase shift angle
Δv_{C1}	Ripples in voltage across capacitor C_1
ΔV_p	Change in SPV voltage
ε	Error between calculated grid voltage and measured grid voltage
κ	Feedforward multiplier constant
λ	Convergence variable in Lyapunov approach
μ	Constant to define hyperbolic tangent thickness
μ_s	Step size of LMS algorithm
ρ	Step size of the least-mean-square (LMS) algorithm
σ	Lyapunov gain parameter
$\varphi(t)$	Phase of the grid voltage
$\varphi_e(t)$	Estimated phase of the grid voltage
χ	Constant in gradient descent method
ψ	Generalized desired signal
ψ_e	Estimated value of desired signal
ψ_o	Initial value of desired signal
ω	Grid frequency
$\omega_1, \omega_2, \omega_3, \omega_4$	Legendre coefficients
ω_c	Grid frequency calculated from PLL
ω_n	nominal grid frequency
$\omega_{n,e}$	Estimated nominal grid frequency
ω_r	resonance frequency
Γ	Lyapunov Constant